

Chelate Effect in the Gas Phase. The Complexes of Ni(2,2,6,6-tetramethyl-3,5-heptanedionate)₂ with Bidentate Ligands

Franzpeter Emmenegger,^{*,†} Carl Wilhelm Schlaepfer,[†] Helen Stoeckli-Evans,[‡] Michel Piccand,[†] and Henryk Piekarski[§]

Inorganic Chemistry, University-Pérolles, CH-1700 Fribourg, Switzerland, Chemistry Department, University of Neuchâtel, Neuchâtel, Switzerland, University of Lodz, Department of Physical Chemistry, Lodz, Poland

Received December 27, 2000

When a bidentate ligand L–L is added to the square planar Ni(tmhd)₂ (tmhd = tetramethylheptanedionate), the octahedral complex Ni(tmhd)₂L–L is formed. This reaction has been studied by vis spectroscopy in toluene at 25 °C and in the gas phase between 150 and 350 °C. It allows the comparison on one hand of the chelate effect of three ligands forming five-membered chelate rings: (i) the flexible N–N ligand tetramethylethylenediamine (TEME); (ii) the rigid N–N ligand 2,2'-bipyridine (BPY); (iii) the flexible N–O ligand dimethylaminomethoxyethane (MAO). On the other hand, it allows the comparison of these ligands with the six-membered chelate ring-forming N–N ligand 1,3-tetramethylpropylenediamine (TEMP). From the temperature dependence of the gas-phase stability constants, enthalpies and entropies of the complex-forming reactions have been derived. As there are no solvation effects in the gas phase, the reaction enthalpies are the metal–ligand bond enthalpies. This is of particular interest for the hemilabile ligand MAO. For the N–N ligands, the stability of the metal–ligand bonds decreases in the order TEME > BPY > TEMP. The entropy of the complex formation with the two flexible ligands TEME and MAO is the same, while it is slightly more positive for the rigid BPY and a lot more positive for TEMP. $\Delta_{\text{form}}G^{\circ}_{298}$ of the complexes is more negative in the gas phase than in solution because the solvation energy of the reactants is more negative than the solvation energy of the products. This is shown in detail for the formation of Ni(tmhd)₂BPY where data of a complete thermodynamic cycle are presented.

1. Introduction

For most chelate complexes—in particular for complexes of first-row transition metals with polyamines—five-membered chelate rings are the most stable ones.^{1,2}

Two concepts are generally referred to to explain the increased stability of chelate complexes as compared to complexes with individual ligands: (i) the closeness of the other ligand atom(s) of the chelate once the first metal ligand bond is formed;³ (ii) the more positive entropy of the formation of the chelate complex.⁴

The first concept is based on geometrical considerations and is rather qualitative.

The second concept is based on the fact that more monodentate ligands are liberated than chelating ligands are used in the reaction. Thus, the number of “free” particles increases and the reaction entropy is positive. The main shortcoming of the concept is that it does not consider changes in solvation intimately associated to the reaction and affecting both its enthalpy and entropy.^{5a,b} This shortcoming has been documented by Myers⁶ who used known thermodynamic data of model

compounds to calculate ΔH° and ΔS° of some metal complex formation reactions in the gas phase and of the solvation of all reaction partners. This allowed him to establish thermodynamic cycles of some complex formation reactions including an analysis of the chelate effect, which clearly showed that the chelate effect is not only an entropy effect. In recent reviews, Breslow⁷ and Yatsimirskii⁸ have again pointed out that the chelate effect is more subtle than a simple entropy-based model could explain. Of particular interest is Breslow's report of the role of the chelate effect in biochemical reactions where there are even examples of a chelate effect based on favorable enthalpy and unfavorable entropy.

While Myers' data of the stability of gaseous metal complexes were based on volatile model compounds, we will address the question of the chelate effect in the gas phase by investigating some volatile metal complexes. The reactions we investigated are represented in Scheme 1. Unfortunately, complexes with two individual ligands such as two pyridines or two dimethylamines are not sufficiently stable for studies at elevated temperatures. But 1,2-bis(dimethylamino)ethane (= tetramethylethylenediamine = TEME) and 1,3-bis(dimethylamino)propane (= tetramethylpropylenediamine = TEMP) allow to compare the stabilities of five- and six-membered chelate rings of two flexible ligands while 2,2'-bipyridine (= BPY) makes a rather rigid five-membered chelate ring. Dimethylaminomethoxyethane (MAO) is a hemilabile ligand.⁹ Complexes of such ligands play a key role in catalysis. While the strongly bond dimethylamino

[†] University-Pérolles.

[‡] University of Neuchâtel.

[§] University of Lodz.

(1) Schwarzenbach, G. *Helv. Chim. Acta* **1952**, *35*, 2344.

(2) Hancock, R. D. *J. Chem. Educ.* **1992**, *69*, 615.

(3) Rosseinsky, D. R. *J. Chem. Soc. Dalton Trans.* **1979**, 732.

(4) Cotton, F. A.; Wilkinson, G. *Advanced Inorganic Chemistry*, 5 ed.; John Wiley & Sons: New York, 1988.

(5) (a) Frausto Da Silva, J. J. R. *J. Chem. Educ.* **1983**, *60*, 390. (b) Gerloch, M.; Constable, E. C. *Transition Metal Chemistry*; VCH Publishers: New York, 1994.

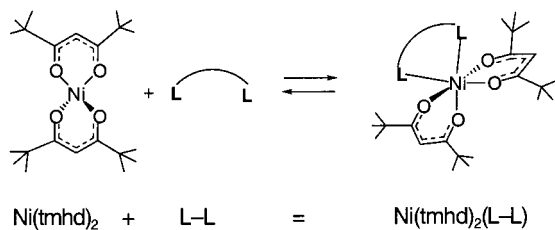
(6) Myers, R. T. *Inorg. Chem.* **1978**, *17*, 952.

(7) Breslow, R.; Belvedere, S.; Gershell, L.; Leung, D. *Pure Appl. Chem.* **2000**, *72*, 333.

(8) Yatsimirskii, K. B. *Russ. Khim. Zh.* **1996**, *40*, 7.

(9) Schneider, J. J. *Nachr. aus Chemie, Wissenschaft und Technik* **2000**, *48*, 614.

Scheme 1



tmhd: 2,2,6,6-tetramethyl-3,5-heptanedionate,

L-L: BPY = 2,2'-bipyridine; TEME = tetramethylethylenediamine;

TEMP = tetramethylpropylenediamine; MAO = 1-dimethylamino-2-methoxy-ethane.

group guarantees the stability of the complex, the weakly bonded ether group is easily replaced allowing catalytic activity. The stability difference of the gaseous complexes $\text{Ni}(\text{tmhd})_2\text{TEME}$ and $\text{Ni}(\text{tmhd})_2\text{MAO}$ gives direct access to the Ni–N and Ni–O bond enthalpies.

2. Experimental Section

2.1. Chemicals. Tmhd (Fluka, purum) and BPY (Fluka, puriss.) were used as received. TEME and TEMP were distilled from solid KOH before use.

MAO was synthesized by reacting 1-chloro-2-(dimethylamino)ethane with sodium methanolate.¹⁰ Purification of the product for a satisfactory elemental analysis was not successful, but the analysis of the sublimed complex $\text{Ni}(\text{tmhd})_2\text{MAO}$ proved it to be pure.

Syntheses of the complexes were analogous to the syntheses of $\text{Co}(\text{tmhd})_2$ and $\text{Co}(\text{tmhd})_2\text{bpy}$ described before.¹¹

2.2. Thermal Analysis. DSC and TG were performed on a Mettler TA 3000 thermal analyzer. Enthalpies of fusion were determined by DSC. Modified entrainment^{12,13} was used to determine the vapor pressures and the decomposition pressures of the complexes.

2.3. Vis Spectroscopy. Spectra in solution (mostly toluene) were measured with a Perkin-Elmer Lambda 2 spectrophotometer and evaluated as described in ref 14.

At elevated temperature (150–350 °C), vis spectra were recorded and evaluated as described in ref 15.

The experimental procedure is exemplified by the system $\text{Ni}(\text{tmhd})_2/\text{TEME}$.

The spectra of eight evacuated ampules (10 cm optical path length) containing different amounts of $\text{Ni}(\text{tmhd})_2$ and TEME were measured in 10 K steps from 250 to 310 °C. The ratio $\text{Ni}(\text{tmhd})_2/\text{TEME}$ varied from 0.2 to 2. $[\text{Ni}(\text{tmhd})_2]_{\text{tot}}$ varied from 0.3 to 1.1 M. For all samples at $T > 250$ °C, the entire contents of the ampule were in the gas phase. Composition and absorbance of the gas phase are described by eqs 1 and 2.

$$K = \frac{[\text{Ni}(\text{tmhd})_2\text{TEME}]}{[\text{Ni}(\text{tmhd})_2][\text{TEME}]} \quad (1)$$

$$A_{\text{tot}} = \epsilon_{[\text{Ni}(\text{tmhd})_2]}[\text{Ni}(\text{tmhd})_2] + \epsilon_{[\text{Ni}(\text{tmhd})_2\text{TEME}]}[\text{Ni}(\text{tmhd})_2\text{TEME}] \quad (2)$$

$\epsilon_{[\text{Ni}(\text{tmhd})_2]}$ is known from the spectrum of pure $\text{Ni}(\text{tmhd})_2(\text{g})$, and $\epsilon_{[\text{Ni}(\text{tmhd})_2\text{TEME}]}$ is known at least approximately from the spectrum of an ampule containing some $\text{Ni}(\text{tmhd})_2$ and 10 times more TEME. As

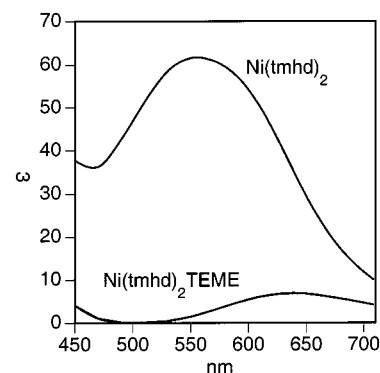


Figure 1. Spectra of $\text{Ni}(\text{tmhd})_2(\text{g})$ and $\text{Ni}(\text{tmhd})_2\text{TEME}(\text{g})$.

$\epsilon_{[\text{Ni}(\text{tmhd})_2\text{TEME}]} \ll \epsilon_{[\text{Ni}(\text{tmhd})_2]}$ $[\text{Ni}(\text{tmhd})_2\text{TEME}]$ contributes little to A_{tot} and it is not important to know $\epsilon_{[\text{Ni}(\text{tmhd})_2\text{TEME}]}$ precisely to calculate $[\text{Ni}(\text{tmhd})_2]$ from A_{tot} , K , $\epsilon_{[\text{Ni}(\text{tmhd})_2]}$, and $\epsilon_{[\text{Ni}(\text{tmhd})_2\text{TEME}]}$ were fitted to reproduce the measured spectra (at 14 wavelengths, 450–709 nm) with minimal error.¹⁵ At every temperature, $8 \times 14 = 112$ data points were available for the fit. Besides the equilibrium constant K , the calculation yields the individual spectra of the two compounds $\text{Ni}(\text{tmhd})_2$ and $\text{Ni}(\text{tmhd})_2\text{TEME}$ in close agreement with the experiments mentioned above (Figure 1).

For $\text{Ni}(\text{tmhd})_2\text{MAO}$, no measurements with excess of L–L could be performed due to lack of pure MAO.

The variation of ϵ with temperature was assumed to be negligible while the temperature dependence of K was used to calculate ΔH° and ΔS° of the complex formation (van't Hoff plot).

2.4. Magnetic Measurements. Susceptibility measurements were performed with a modified Gouy balance by Sherwood Scientific Ltd., Cambridge GB. $\text{Ni}(\text{tmhd})_2$ is diamagnetic ($\mu_{\text{eff}} = 0 \mu_B$), and $\text{Ni}(\text{tmhd})_2\text{L-L}$ is paramagnetic corresponding to an octahedral high spin d^8 configuration ($\mu_{\text{eff}} = 2.9\text{--}3.0 \mu_B$).

2.5. X-ray Data Collection and Structure Solution. Pale blue blocklike crystals of $\text{Ni}(\text{tmhd})_2\text{TEME}$ (ca. $0.40 \times 0.40 \times 0.40$ mm), $\text{Ni}(\text{tmhd})_2\text{TEMP}$ (ca. $0.35 \times 0.25 \times 0.20$ mm), and $\text{Ni}(\text{tmhd})_2\text{MAO}$ (ca. $0.50 \times 0.40 \times 0.30$ mm) were mounted on a Stoe imaging plate diffractometer system²² equipped with a one-circle φ goniometer and a graphite monochromator. Data collections were performed at 223 K using Mo $K\alpha$ radiation ($\lambda = 0.71073 \text{ \AA}$). Two hundred exposures (3 min per exposure) were obtained at an image plate distance of 70 mm (resolution $D_{\text{min}} - D_{\text{max}}$ 14.23–0.87 \AA) with $0 < \varphi < 200^\circ$ and the crystal oscillating through 1° in φ . The structures were solved by direct methods using the program SHELXS-97¹⁶ and refined by full-matrix least-squares methods on F^2 with SHELXL-97.¹⁷ The hydrogen atoms were included in calculated positions and treated as riding atoms using SHELXL-97 default parameters. Crystallographic data for $\text{Ni}(\text{tmhd})_2\text{TEME}$, $\text{Ni}(\text{tmhd})_2\text{TEMP}$, and $\text{Ni}(\text{tmhd})_2\text{MAO}$ are summarized in Table 1. In all three compounds, the *tert*-butyl groups either undergo considerable thermal motion or were disordered, and two alternative positions were found for the methyl groups. In some cases, it was necessary to restrain the C–CH₃ bonds to be 1.54(1) \AA . In $\text{Ni}(\text{tmhd})_2\text{TEMP}$, the propylenediamine ligand is disordered. Further details are given in the crystallographic CIF files (Supporting Information). The perspective view of $\text{Ni}(\text{tmhd})_2\text{TEME}$ (Figure 5) was drawn using the program PLATON.¹⁸

2.6. Errors and Uncertainties. For most thermodynamic values there are not enough independent measurements to compute valid random errors. Determinate errors of individual measurements are difficult to estimate. Nevertheless, some indication about probable limits of error of our results shall be given.

Equilibrium constants of gas-phase reactions are estimated to have an error of less than a factor of 3, yielding an uncertainty of ± 2.5 kJ

(10) Grahl G. F.; Tenenbaum, L. E.; Tolstoonhov, A. V.; Duca, C. J.; Reihard, J. F.; Anderson, F. E.; Scudi, J. V. *J. Am. Chem. Soc.* **1952**, *72*, 1313.

(11) Chassot, P.; Emmenegger, F. P. *Inorg. Chem.* **1996**, *35*, 5931.

(12) Emmenegger, F. P.; Piccand M. *Z. Anorg. Allg. Chem.* **1993**, *619*, 17.

(13) Emmenegger, F. P.; Piccand M. *J. Therm. Anal. Cal.* **1999**, *57*, 235.

(14) Emmenegger, F. P.; Piccand, M.; Piekarski, H.; Mokrzan J. *J. Chem. Soc., Dalton Trans.* **1997**, 785.

(15) Daul, C.; Emmenegger, F. P.; Mlinar, M.; Piccand, M. *Inorg. Chem.* **1993**, *32*, 2992.

(16) Sheldrick, G. M. *Acta Cryst.* **1990**, *A46*, 467–473.

(17) Sheldrick, G. M. *SHELXL-97, Program for crystal structure refinement*; University of Göttingen, Germany, 1997.

(18) Spek, A. L. PLATON/PLUTON, version Jan. 1999. *Acta Crystallogr.* **1990**, *A46*, C34.

Table 1. Crystallographic Data for Ni(tmhd)₂TEME, Ni(tmhd)₂TEMP, and Ni(tmhd)₂MAO

	Ni(tmhd) ₂ TEME	Ni(tmhd) ₂ TEMP	Ni(tmhd) ₂ MAO
chem formula	C ₂₈ H ₅₄ N ₂ NiO ₄	C ₂₉ H ₅₆ N ₂ NiO ₄	C ₂₇ H ₅₁ NNiO ₅
formula wt	541.4	555.5	528.4
space group	<i>P2₁/n</i>	<i>P2₁/n</i>	<i>P2₁/c</i>
<i>a</i> , Å	10.016(1)	10.097(1)	13.626(1)
<i>b</i> , Å	18.927(1)	19.001(2)	12.079(1)
<i>c</i> , Å	17.194(2)	17.251(1)	19.440(2)
β , °	92.96(1)	91.38(1)	103.96(1)
<i>V</i> , Å ³	3255.1(4)	3308.8(4)	3105.0(5)
<i>Z</i>	4	4	
λ , Å	0.71073	0.71073	
ρ_{calcd} , g cm ⁻³	1.105	1.115	1.130
μ , cm ⁻¹	6.26	11.15	6.56
^a <i>R</i> (<i>F</i> _o)	0.0482	0.0460	0.0433
obsd data			
^b wR2(<i>F</i> _o ²), all data	0.1430	0.1161	0.1295

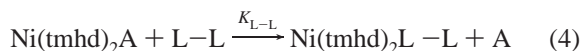
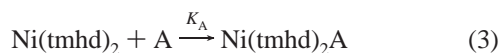
$${}^a R = \sum ||F_o| - |F_c|| / \sum |F_o|. \quad {}^b wR2 = (\sum [w(F_o^2 - F_c^2)^2]) / \sum [w(F_o^2)^2]^{1/2}.$$

mol⁻¹ for ΔG°_{550K} and of ± 1.5 J mol⁻¹ for ΔG°_{298K} . ΔH values from calorimetric measurements are estimated to be uncertain by $\pm 3\%$, but the uncertainty of ΔH° from van't Hoff plots is certainly larger; we assume it to be $\pm 6\%$. ΔS° from van't Hoff plots has an estimated uncertainty of $\pm 20\%$. Solubilities are at least accurate within a factor of 2 yielding an uncertainty of ± 1 kJ mol⁻¹ for the ΔG° of the dissolution reaction. The accuracy of the stability constants in solution is discussed in 3.1.

3. Results

3.1. Stability of Ni(tmhd)₂L–L in Solution. Addition of a bidentate ligand to the low-spin diamagnetic square-planar Ni(tmhd)₂ produces a paramagnetic octahedral complex and thus reduces the absorbance in the visible. The stability of the complexes can therefore be determined by vis spectroscopy. The spectra in solution are very similar to those in the gas phase, Figure 1.

In solution, the stability constants K_1 of the complexes formed according to Scheme 1 are so large that addition of L–L to Ni(tmhd)₂ produces almost 100% of Ni(tmhd)₂L–L and the denominator in the mass action law approaches zero. Therefore, the formation constant of Ni(tmhd)₂L–L cannot be determined by recording spectrophotometrically the titration of a solution of Ni(tmhd)₂ with L–L. The problem could be partially solved by using a stepwise procedure. In a first step, the smaller (and therefore spectrophotometrically measurable) stability constants of Ni(tmhd)₂A, reaction 3, were determined (A = 1,2-bis-(diphenylphosphino)ethane or 1,2-dimethoxyethane or two pyridines). Then the substitution equilibria of A by L–L were measured, reaction 4. The product $K_A \times K_{L-L}$ equals the stability constant K_1 according to Scheme 1.



Even so, only the order of magnitude (estimated uncertainty: $\log K_1 \pm 1$) and the relative stability of the complexes could be established (Table 2).

3.2. Stability of Ni(tmhd)₂L–L in the Gas Phase. 3.2.1. Vapor Pressure Measurements. Evaporation measurements on a thermobalance showed that all the complexes (Ni(tmhd)₂L–L) evaporate congruently; i.e., they pass into the vapor phase as a whole. The vapor pressure could therefore be measured by “modified entrainment”¹³ (Table 3).

3.2.2. Gas-Phase Equilibria. The equilibrium constant of reaction 5 can be determined by measuring the absorbance of

Table 2. Stability of Ni(tmhd)₂L–L in Toluene

A ^a	log <i>K_A</i>	L–L	log <i>K_{L–L}</i>	log(<i>K_A</i> × <i>K_{L–L}</i>) = log <i>K₁</i>
py	4.03			
2py	7.97 (β_2)	bpy	0.53	8.5
dppe	4.56	bpy	3.02	7.6
dppe	4.56	TEME	4.85	9.4
dmoe	2.0	TEME	6.7	8.7
bpy	8.0	TEME	2.9	10.9
bpy	8.0	MAO	−1	7.0
bpy	8.0	TEMP	−0.3	7.7
dmoe	2	TEMP	4.8	6.8

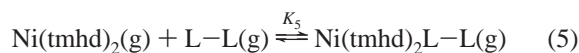
^a dppe = 1,2-bis-(diphenylphosphino)-ethane. dmoe = 1,2-dimethoxyethane.

Table 3. Thermochemical Data of the Complexes Ni(tmhd)₂L–L^a

compd	mp (°C)	$\Delta_{\text{melt}}H^\circ$ (kJ mol ⁻¹)	$\Delta_{\text{evap}}H^\circ$ (kJ mol ⁻¹)	$\Delta_{\text{evap}}S^\circ$ (J mol ⁻¹ K ⁻¹)
Ni(tmhd) ₂	228	39	110 (subl)	160 (subl)
Ni(tmhd) ₂ BPY	243	38	131 (subl)	183 (subl)
Ni(tmhd) ₂ BPY			92	105
Ni(tmhd) ₂ TEME	163	21	89	121
Ni(tmhd) ₂ TEMP	166	22	122	198
Ni(tmhd) ₂ MAO	116	29	64	76
TEME			37	69
BPY	see Table 5			

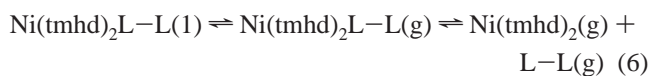
^a Standard state: mol L⁻¹.

cells where known amounts of Ni(tmhd)₂ and L–L are completely evaporated. The evaluation



of such measurements by principal component analysis is described in ref 15 (see the Experimental Section). Table 4 lists the thermodynamic parameters for equilibrium (5) and—for comparison— $\Delta_f G^\circ_{298}$ of the complexes in toluene. Figure 2 shows the van't Hoff plots of equilibrium (5) for the various ligands used in the study.

The gas-phase equilibrium (5) obviously also holds if one of the reaction partners is also present as a solid or liquid. Therefore, vapor pressures calculated from data of Table 3 (from modified entrainment) and the equilibrium constants calculated from the data of Table 4 allow the computation of the relative concentrations of Ni(tmhd)₂(g) and Ni(tmhd)₂L–L(g) in equilibrium with liquid (or solid) Ni(tmhd)₂L–L as shown by the equilibria (6).



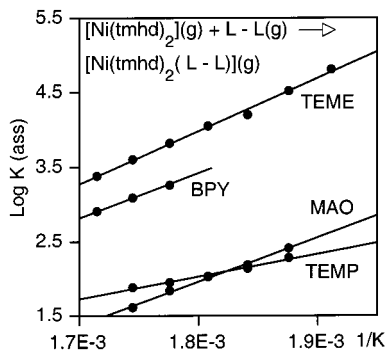
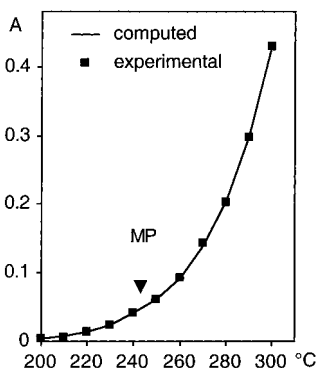
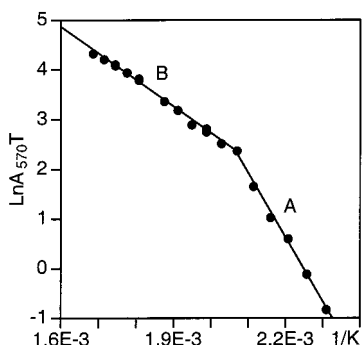
Considering the experimental conditions in our optical cells, the congruently evaporating Ni(tmhd)₂BPY yields an equilibrium mixture of around 50% of Ni(tmhd)₂(g) and 50% of Ni(tmhd)₂BPY(g). At 570 nm, $\epsilon_{[\text{Ni(tmhd)}_2]} = 63 \pm 1$ M⁻¹ cm⁻¹ and $\epsilon_{[\text{Ni(tmhd)}_2\text{BPY}]} \approx 2 \pm 0.5$ M⁻¹ cm⁻¹; i.e., the absorbance of the gas is essentially due to Ni(tmhd)₂ (see Figure 1, spectra of the similar pair of complexes Ni(tmhd)₂ and Ni(tmhd)₂TEME). Figure 3 shows that the computed absorbance at 570 nm fits the experimental points well. The same is true for the other complexes Ni(tmhd)₂L–L.

Another test of the data consists of plotting $\ln AT = f(1/T)$ while heating Ni(tmhd)₂L–L. Ni(tmhd)₂TEME is used as an example. Two straight lines are obtained (Figure 4). Below 265 °C, [Ni(tmhd)₂] is due to equilibria (6) while the absorbance above 265 °C is governed by [Ni(tmhd)₂](g) in equilibrium (5). Part A of the graph can indeed be exactly reproduced by combining the data of the “modified entrainment” vapor pressure measurements (Table 3) with the data for equilibrium (5) (Table 4), while section B corresponds to the Ni(tmhd)₂ equilibrium

Table 4. Thermodynamic Data of the Gas-Phase Reaction 5 and the Corresponding Reaction in Toluene^a

L-L	$\Delta_r H^\circ$ (550 K) (kJ mol ⁻¹)(g)	$\Delta_r S^\circ$ (550 K) (J mol ⁻¹ K ⁻¹)(g)	$\Delta_r G^\circ$ (550 K) (kJ mol ⁻¹)(g)	$\Delta_r G^\circ$ (298 K) (kJ mol ⁻¹) calcd (g)	$\Delta_r G^\circ$ (298 K) (kJ mol ⁻¹) measured (d) ^b
BPY	-110	-133	-37	-70	-46 ± 6
TEME	-136	-169	-43	-85	-55 ± 6
TEMP	-58	-66	-22	-38	-42 ± 6
MAO	-114	-167	-22	-64	-40 ± 6
2py					-45 ± 1

^a Standard state: mol L⁻¹. ^b Error limits for $\Delta_r G^\circ$ (298K) in toluene see Table 2.

**Figure 2.** Van't Hoff plot for reactions 5.**Figure 3.** A_{570} when $\text{Ni}(\text{tmhd})_2\text{BPY}$ is heated. Points: experimental. Line: calculated from data of Tables 3–5.**Figure 4.** Figure 4. Van't Hoff plot for the equilibria (6): $\text{Ni}(\text{tmhd})_2\text{TEME}(l) \rightleftharpoons \text{Ni}(\text{tmhd})_2\text{TEME}(g) \rightleftharpoons \text{Ni}(\text{tmhd})_2(g) + \text{TEME}(g)$. A: gas phase in equilibrium with $\text{Ni}(\text{tmhd})_2\text{TEME}(l)$. B: gas phase only.

pressure (Table 4) after complete evaporation of the $\text{Ni}(\text{tmhd})_2\text{TEME}$ sample.

3.3. Structure of the Complexes. Metal–ligand bond distances and angles are listed in Table 6. It shows that the Ni–O distance of the Ni–tmhd unit is independent of the ligand L–L. The geometries of $\text{Ni}(\text{tmhd})_2\text{TEME}$ and $\text{Ni}(\text{tmhd})_2\text{MAO}$ are almost the same, while in $\text{Ni}(\text{tmhd})_2\text{TEMP}$ the Ni–N distance and the N–Ni–N angle are larger and the larger L–L ligand pushes the tmhd ligands closer to each other as shown by the smaller O_2NiO_3 angle.

Table 5. Data for Thermodynamic Cycle of Scheme 2^a

no.	reaction	ΔH° (kJ mol ⁻¹)	ΔS° (kJ mol ⁻¹ K ⁻¹)	ΔG° 298 K (kJ mol ⁻¹)
1	association in the gas phase	-110	-133	-70
2	association in solution	-65 ^b	-64	-46
3	dissolution of $\text{Ni}(\text{tmhd})_2(\text{s})$	32 ^c	86	6
4	sublimation of $\text{Ni}(\text{tmhd})_2$	110	160	62
5	dissolution of BPY(s)	19 ^c	72	-2
6	sublimation of BPY	75 ^d	128	37
7	dissolution of $\text{Ni}(\text{tmhd})_2\text{BPY}$	22 ^c	50	7
8	sublimation of $\text{Ni}(\text{tmhd})_2\text{BPY}$	131	183	76
	$ \Sigma $	20	72	2

^a Standard state: 1 mol L⁻¹. ^b Enthalpometric titration, see ref 11. ^c Calorimetry, see ref 11. ^d Converted to standard state 1 bar: 78 kJ mol⁻¹ (ref 20: 81.8 ± 2.3 kJ mol⁻¹).

Table 6. Bond Distances (pm) and Angles in $\text{Ni}(\text{tmhd})_2\text{L-L}^a$

	TEME	TEMP	MAO
Ni–O ₁	201.75	200.5	200.68
Ni–O ₂	200.10	202.0	199.68
Ni–O ₃	199.38	201.6	199.55
Ni–O ₄	202.07	201.3	200.09
Ni–N ₁	216.3	220.1	215.2
Ni–N ₂	216.6	220.9	(O) 216.39
O ₁ NiO ₂	89.10	89.31	89.39
O ₃ NiO ₄	89.42	89.61	90.98
O ₂ NiO ₃	93.48	87.38	94.38
N ₁ NiN ₂ (O)	83.46	93.39	(O) 81.05

^a For atom numbers, see Figure 5.

4. Discussion

Vapor pressure data of the investigated complexes may be of some interest to research using such complexes as source materials for the chemical vapor deposition (CVD) of nickel compounds,¹⁹ but we will not discuss this aspect of our work.

The structures of the four complexes we have investigated are very similar; an ORTEP plot of $\text{Ni}(\text{tmhd})_2\text{TEME}$ is shown in Figure 5 as a representative example. Further details are available in the Supporting Information.

For $\text{Ni}(\text{tmhd})_2\text{BPY}$, the data of the complete thermodynamic cycle, Scheme 2, are presented in Table 5.

The sum of the individual contributions of the cycle should obviously be zero. This is almost so for the free energies, $\Sigma\Delta G^\circ = 2$ kJ mol⁻¹, while for the enthalpies an uncertainty of 7% for the individual contribution has to be admitted, $\Sigma\Delta H^\circ = 20$ kJ mol⁻¹. Entropies from van'tHoff plots are notoriously less precise than enthalpies. In the cycle, $\Sigma\Delta S^\circ = 72$ J mol⁻¹ K⁻¹, leading to an uncertainty of 21% for the individual contribution.

For the $\text{Co}(\text{tmhd})_2\text{BPY}$, the data corresponding to Scheme 2 have been published.¹¹ The enthalpy of reaction 1 of Scheme 2, -110 kJ mol⁻¹, corresponding to the Ni–BPY bond energy, is significantly more negative than the corresponding Co–BPY bond energy, -98 kJ mol⁻¹, in agreement with the generally observed stability trend of the first-row transition-metal complexes (Irving–Williams rule²¹).

(19) Wang, A.; Belot, O. A.; Marks, T. J. *J. Mater. Res.* **1999**, *14*, 1132.

(20) Ribeiro de Silva, M. A. V.; Morais, V. M. F.; Matos, M. A. R.; Rio, C. M. A. *J. Org. Chem.* **1995**, *60*, 5291.

(21) Irving, H.; Williams, R. J. P. *J. Chem. Soc.* **1953**, 3192.

(22) Stoe & Cie. IPDS Software; Stoe & Cie GmbH: Darmstadt, Germany, 2000.

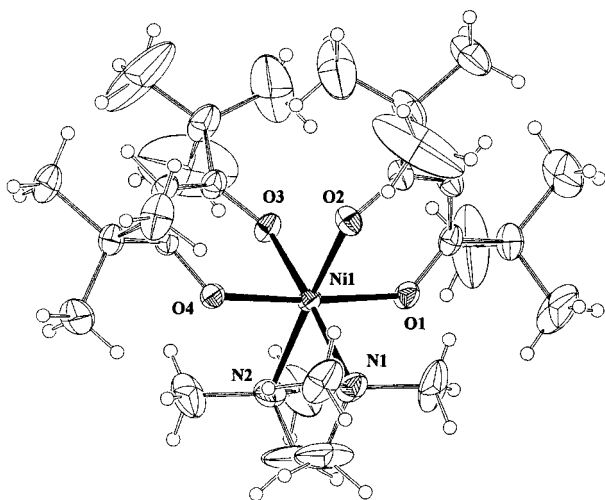
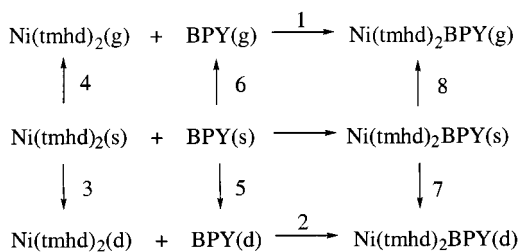


Figure 5. Perspective view¹⁸ of Ni(tmhd)₂TME; thermal ellipsoids at 30% probability level.

Scheme 2

Thermodynamic cycle



The enthalpy of solvation of Ni(tmhd)₂BPY (−109 kJ mol^{−1}) equals the enthalpy of the complex formation (−110 kJ mol^{−1}) illustrating the importance of solvation in metal complex formation. Nevertheless, solvation energies are, in general, not considered when complex stabilities are discussed⁵ because the corresponding data are scarce.

Extrapolation of $\Delta_f G^\circ$ in the gas phase from 550 to 298 K (neglecting the temperature dependence of ΔH° and ΔS°) indicates that the complexes are more stable in the gas phase than in solution (except for Ni(tmhd)₂TEMP where $\Delta_{\text{form}} G^\circ_{298}(\text{g}) \approx \Delta_{\text{form}} G^\circ_{298}(\text{d})$, Table 4). This implies that the solvation energy of the reactants is larger (more negative) than the one of the products. For the formation of Ni(tmhd)₂BPY where solvation energy data are available, it appears that it is mostly the solvation energy of BPY that stabilizes the reactants in favor of the products. It might be assumed that the situation is similar for the other L–L ligands of this study.

The flexible ligands TME and MAO form five-membered chelate rings. In agreement with the concept of Rosseinsky,³ their entropy of formation is the same, but the TME complex is more stable than the MAO complex because the bond energy Ni–N is larger than the bond energy Ni–O. The Ni–N distance is very similar in Ni(tmhd)₂TME and in Ni(tmhd)₂MAO (Table 6), and it is therefore justified to assume the same Ni–N bond energy in both complexes (−68 kJ mol^{−1}). This yields −46 kJ

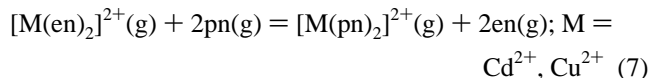
mol^{−1} for the Ni–O bond in Ni(tmhd)₂MAO. It should be mentioned that the weaker Ni–O bond, as compared to the Ni–N bond, is not due to a longer Ni–O distance; the Ni–O bond has the same length as the Ni–N bond (Table 6). The large difference (22 kJ mol^{−1}) between the bond energies of Ni–N and Ni–O is responsible for the hemilabile⁹ character of MAO. To our knowledge, this is the first experiment that gives direct quantitative information about the hemilabile character of a ligand.

As one might have expected, the entropy of the complex formation with the flexible ligands TME and MAO is more negative than with the more rigid ligand BPY.

In the gas phase, at 550 K, as well as in toluene the two complexes Ni(tmhd)₂TEMP and Ni(tmhd)₂MAO have the same stability, i.e., the smaller chelate effect of the six-membered chelate ring of TEMP has the same effect on the stability as the switch from an amine ligand in Ni(tmhd)₂TME to an ether ligand in Ni(tmhd)₂MAO.

For the complexes with only nitrogen donors—TME, BPY, and TEMP—the stability sequence in the gas phase and in solution is the same but due to solvation the differences are attenuated in solution.

A thermodynamic analysis of the stability difference of dissolved complexes with ethylenediamine and propylenediamine by Hancock² has shown that the greater stability of the five-membered chelate ring as compared to the six-membered ring is mostly due to the more negative enthalpy of complex formation with the former. From Myers'⁶ data, the enthalpy of the exchange of ethylenediamine (en) by propylenediamine (pn) in the gas phase, reaction 7, can be calculated: $\Delta H^\circ_{(7)} = 17.1$ kJ mol^{−1}.



We observe a much larger enthalpy for the exchange of one TME by one TEMP on Ni(tmhd)₂L–L (78 kJ mol^{−1}, Table 4).

X-ray structure determinations of the solids indicate that TEMP in Ni(tmhd)₂TEMP is fluxional with a slightly longer Ni–N distance than in Ni(tmhd)₂TME (Table 6). This again explains why the Ni–N bond energy is considerably smaller in Ni(tmhd)₂TEMP than in Ni(tmhd)₂TME and why the entropy of the complex formation of Ni(tmhd)₂TEMP is less negative than for the other L–L ligands.

Acknowledgment. We thank Dr. Nagwa Ghoneim, Institute of Physical Chemistry, University of Fribourg, for performing the enthalpometric titration. This work is part of Project 20-40641.94 of the Swiss National Science Foundation.

Supporting Information Available: Tables of crystal data, structure refinement, atomic positional parameters, anisotropic thermal parameters, hydrogen atoms positions, full bond distances and angles, and torsion angles for Ni(tmhd)₂TME, Ni(tmhd)₂TEMP, and Ni(tmhd)₂MAO. This material is available free of charge via the Internet at <http://pubs.acs.org>

IC0014540